Aquatic Toxicology 227 (2020) 105582

Contents lists available at ScienceDirect

Aquatic Toxicology

journal homepage: www.elsevier.com/locate/aqtox

Combined effects of exposure to engineered silver nanoparticles and the water-soluble fraction of crude oil in the marine copepod *Calanus finmarchicus*

J. Farkas[a,*,1], V. Cappadona[a,2], A.J. Olsen[a], B.H. Hansen[b], W. Posch[c], T.M. Ciesielski[a], R. Goodhead[d], D. Wilflingseder[c], M. Blatzer[c], D. Altin[e], Julian Moger[f], A.M. Booth[b], B.M. Jenssen[a]

[a] Department of Biology, Norwegian University of Science and Technology, 7491 Trondheim, Norway
[b] SINTEF Ocean, Environment and New Resources, Trondheim, Norway
[c] Division of Hygiene and Medical Microbiology, Innsbruck Medical University, Innsbruck, Austria
[d] Department for Bioscience, University of Exeter, UK
[e] BioTrix, Trondheim, Norway
[f] Physics and Medical Imaging, College of Engineering, Mathematics and Physical Sciences, University of Exeter, Exeter, Devon, EX4 4QL, United Kingdom

ARTICLE INFO

Keywords:
Silver
Nanoparticles
Oxidative stress
Mixture toxicity
Bioavailability

ABSTRACT

While it is likely that ENPs may occur together with other contaminants in nature, the combined effects of exposure to both ENPs and environmental contaminants are not studied sufficiently. In this study, we investigated the acute and sublethal toxicity of PVP coated silver nanoparticles (AgNP) and ionic silver (Ag^+; administered as $AgNO_3$) to the marine copepod *Calanus finmarchicus*. We further studied effects of single exposures to AgNPs (nominal concentrations: low 15 μg L^{-1} NPL, high 150 μg L^{-1} NPH) or Ag^+ (60 μg L^{-1}), and effects of co-exposure to AgNPs, Ag^+ and the water-soluble fraction (WSF; 100 μg L^{-1}) of a crude oil (AgNP + WSF; Ag^+ + WSF). The gene expression and the activity of antioxidant defense enzymes SOD, CAT and GST, as well as the gene expression of HSP90 and CYP330A1 were determined as sublethal endpoints. Results show that Ag^+ was more acutely toxic compared to AgNPs, with 96 h LC_{50} concentrations of 403 μg L^{-1} for AgNPs, and 147 μg L^{-1} for Ag^+. Organismal uptake of Ag following exposure was similar for AgNP and Ag^+, and was not significantly different when co-exposed to WSF. Exposure to AgNPs alone caused increases in gene expressions of GST and SOD, whereas WSF exposure caused an induction in SOD. Responses in enzyme activities were generally low, with significant effects observed only on SOD activity in NPL and WSF exposures and on GST activity in NPL and NPH exposures. Combined AgNP and WSF exposures caused slightly altered responses in expression of SOD, GST and CYP330A1 genes compared to the single exposures of either AgNPs or WSF. However, there was no clear pattern of cumulative effects caused by co-exposures of AgNPs and WSF. The present study indicates that the exposure to AgNPs, Ag^+, and to a lesser degree WSF cause an oxidative stress response in *C. finmarchicus*, which was slightly, but mostly not significantly altered in combined exposures. This indicated that the combined effects between Ag and WSF are relatively limited, at least with regard to oxidative stress.

1. Introduction

Rapid progression in the field of nanotechnology has led to an increased usage of engineered nanomaterials (ENPs) and their application within nano-enabled consumer products. Despite the continued increase in production volumes of ENPs, concern remains regarding their impact on the environment and human health (Falkner and Jaspers, 2012; Hadrup et al., 2018; Warheit, 2018). Release of ENP to the environment can occur all along the material value chain, including accidental spills, during the use or application of ENP-containing products as well as during waste processing at product end of life (Mueller and Nowack, 2008).

Silver nanoparticles (AgNP) are one of the most widely produced ENPs, and are used in a wide application range, that includes consumer

* Corresponding author at: SINTEF Ocean, Brattørkaia 17C, 7010 Trondheim, Norway.
E-mail address: julia.farkas@sintef.no (J. Farkas).
[1] Current address: SINTEF Ocean, Environment and New Resources, Trondheim, Norway.
[2] Current address: Department of Civil and Environmental Engineering, University of Strathclyde, Glasgow, UK.

https://doi.org/10.1016/j.aquatox.2020.105582
Received 18 April 2020; Received in revised form 13 July 2020; Accepted 18 July 2020
Available online 24 July 2020

products (Benn and Westerhoff, 2008; Farkas et al., 2011), the preparation of oil-based nanofluids (Li et al., 2010) and water purification systems (Dankovich and Gray, 2011; Sun et al., 2015). However, the toxicity of AgNP has been documented for several marine and freshwater species, including bacteria, copepods and fish (Farmen et al., 2012; Navarro et al., 2008; Ribeiro et al., 2014).

Despite the potential benefits gained through use of ENPs, their increasing use may lead to the release into the environment. This can lead to interactions with chemicals which possibly causes mixture effects in organisms either through NPs acting as carriers for various organic and inorganic pollutants or through combined stressor effects (Hartmann and Baun, 2010; Naasz et al., 2018). ENP-contaminant interactions have been shown in several studies, while type of interactions and effects on organisms (bioaccumulation and/or toxicity) are yet poorly understood, as reviewed by Deng et al. (2017). The available data suggest that several ENPs, including carbon nanotubes, TiO_2 NPs and fullerenes (C_{60}), can facilitate the uptake and/or effects of contaminants to aquatic organisms, including marine gastropods, fish, freshwater algae and copepods (Baun et al., 2008; Canesi et al., 2014; Farkas et al., 2015; Glomstad et al., 2016; Park et al., 2019; Sun et al., 2007; Zhang et al., 2007; Zhu et al., 2011). In contrast, several studies report no increase, or even reduced effects in combined exposures (Rosenfeldt et al., 2014, Rosenfeldt et al., 2015). For example, similar or reduced effects of 17α-ethinylestradiol were reported in fish in co-exposures with AgNPs (Farkas et al., 2017). In a recent review, 7 different categories were proposed to describe interactions between nanoparticles and chemicals and implications for bioavailability and toxicity. These categories, namely, Trojan-horse (+), Trojan-horse (-), surface enrichment, retention, inertism and coalism, range from no changes in chemical accumulation and toxicity in the presence of ENPs to either reduced or an increased toxicity, which can be independent or related to changes in uptake and accumulation (Naasz et al., 2018).

The aim of this study was to determine whether combined exposures of AgNP and the water-soluble fraction of oil (WSF) cause altered effects compared to single exposures in a marine copepod. We thus studied oxidative stress effects of AgNP, Ag^+ and WSF of a North Sea of a crude oil using *Calanus finmarchicus* (Gunnerus) as study species. We further investigated the acute toxicity of AgNP and Ag^+.

C. finmarchicus is the most common zooplankton species in the North Atlantic and western part of the Barents Sea and can seasonally account for up to 90 % of the zooplankton biomass (Sakshaug et al., 1992). It is a key species in the sub-Arctic food chain, feeding on phytoplankton blooms in spring and summer, whilst serving as a vital nutrient source and lipid and energy pool for fish and fish larvae, including their main prey species Atlantic cod juveniles (*Gadus morhua*) and Atlantic herring (*Clupea harengus*) (Sakshaug et al., 1992).

2. Material and methods

2.1. Test materials and characterization

Sterically coated (polyvinylpyrrolidone; PVP, 1 wt.%) AgNPs with a nominal average size of 20 nm were purchased in aqueous dispersion from Particular GMBH (Particular GmbH, Hannover, Germany) at a concentration of 100 mg L^{-1}. PVP (PVP10) was purchased from Sigma Aldrich. $AgNO_3$ was used as source for Ag^+ and purchased from Sigma Aldrich. As crude oil, a naphthenic crude oil originating from the Norwegian continental shelf in the North Sea was used.

AgNP size and shape were determined using transmission electron microscopy (TEM) as described in Farkas et al. (2017). Briefly, 100 µL of the AgNP stock dispersion was applied to carbon coated copper grids (200 nm mesh) and particle attachment allowed to occur for several minutes before the remaining liquid was carefully removed to prevent drying artefacts. TEM images were then taken with a Zeiss Libra 120 EF TEM (Carl Zeiss AG, Germany). The hydrodynamic diameter (HDD), polydispersity index (PDI) and zeta potential (ZP) of the AgNP stock (diluted to 10 mg L^{-1} in MQ water) was determined with a Zetasizer ZS (Malvern Instruments, UK) using a 173° backscatter angle. Changes in AgNP absorption were determined as a measure of AgNP stability in seawater over time. AgNP dispersions of 10 mg L^{-1} were prepared in filtered (100 nm) seawater and the absorbance at λ_{max} determined with a UV–vis spectrometer (Lambda 40 UV–vis Spectrometer, Perkin Elmer, Waltham, USA) after 0, 1, 2, 6 and 12 h. To determine the dissolution of Ag^+ from AgNP in seawater, AgNP dispersions (n = 3) of 445 µg L^{-1} (representing the determined LC_{50} concentration; see below) were prepared and gently agitated for 0, 12, 72 and 96 h at 10 °C in darkness. The dispersions were then centrifuged for 1 h at 20 000 rpm in a Sorvall® ultracentrifuge (Thermo Fisher Scientific, Waltham, USA). 10 mL of supernatant were withdrawn, acidified with 0.1 M ultrapure HNO_3 and analyzed for Ag concentration (^{109}Ag and ^{107}Ag) with high resolution inductively coupled plasma mass spectrometry (HR-ICP-MS) with a Thermo Finnigan model Element 2 instrument (Bremen, Germany) applying an SC-FAST flow injection analysis system (ESI, Elemental Scientific, Inc. Ohama, USA). Details on instrument settings, quality control and analyses are described in the supplementary information (S1.1).

2.2. Acute Ag toxicity test

Calanus finmarchicus (Gunnerus) were obtained from a continuous laboratory culture established from the local *C. finmarchicus* population in Trondheimsfjord, Norway and kept under conditions as described previously (Hansen et al., 2007). The copepods used in this study were newly molted non-ovulating females and were from the same generation and culture tank.

A 96 h static acute toxicity experiment was performed to comparatively investigate the LC_{50} of AgNP and Ag^+ on *C. finmarchicus*. The experiments were conducted in 500 mL borosilicate glass flasks capped with Teflon-lined screw caps. Exposure concentrations ranged from 0.040 mg L^{-1} to 2.449 mg L^{-1} for AgNP and 0.018 mg L^{-1} to 0.78 mg L^{-1} for Ag^+ (applied as $AgNO_3$; 0.020–1.230 mg L^{-1}). As positive control, 0.85 mg L^{-1} 3,5-dichlorophenol was included and seawater containing the maximum possible freshwater dilutions without test substances was included as a negative control. Each exposure concentration, including the positive control, was run in triplicate, with 7 copepods per replicate. Six parallels were run in the negative control series. The temperature of test medium was in equilibrium with ambient temperature of the test system (10 ± 2 °C). Exposure was performed under dimmed light conditions and the test animals were not fed during exposure. After 24, 48, 72 and 96 h of exposure, the number of lethally immobilized copepods in each test vessel was scored. To validate exposure concentrations and stability in concentration over time, water samples from all concentrations were taken at the start and end of the test for both Ag^+ and AgNP. Samples of 10 mL were taken from exposure vessels, stabilized with ultrapure 0.1 M HNO_3 and subsequently analyzed for Ag by HR-ICP-MS as described above.

2.3. Combined Ag-WSF exposure experiment

2.3.1. Exposure setup

A continuous flow-through exposure setup was used for the sublethal exposure of *C. finmarchicus* (Fig. 1). The exposure system and experimental tanks have previously been described in detail (Nordtug et al., 2011). In brief, 5 L borosilicate glass bottles were used as exposure tanks, each containing 150 individuals of newly molted non-ovulating females (approximate age of 50 days) of *C. finmarchicus*. The animals were exposed separately to AgNPs, Ag^+, the WSF of the crude oil and mixtures of Ag and WSF. The nominal concentrations of AgNPs were 15 µg L^{-1} (low exposure; NPL) and 150 µg L^{-1} (high exposure; NPH), 60 µg L^{-1} for Ag^+, and 100 µg L^{-1} for WSF.

Negative controls were receiving filtered sea water only. PVP background controls (1 g L^{-1}) were included to determine potential

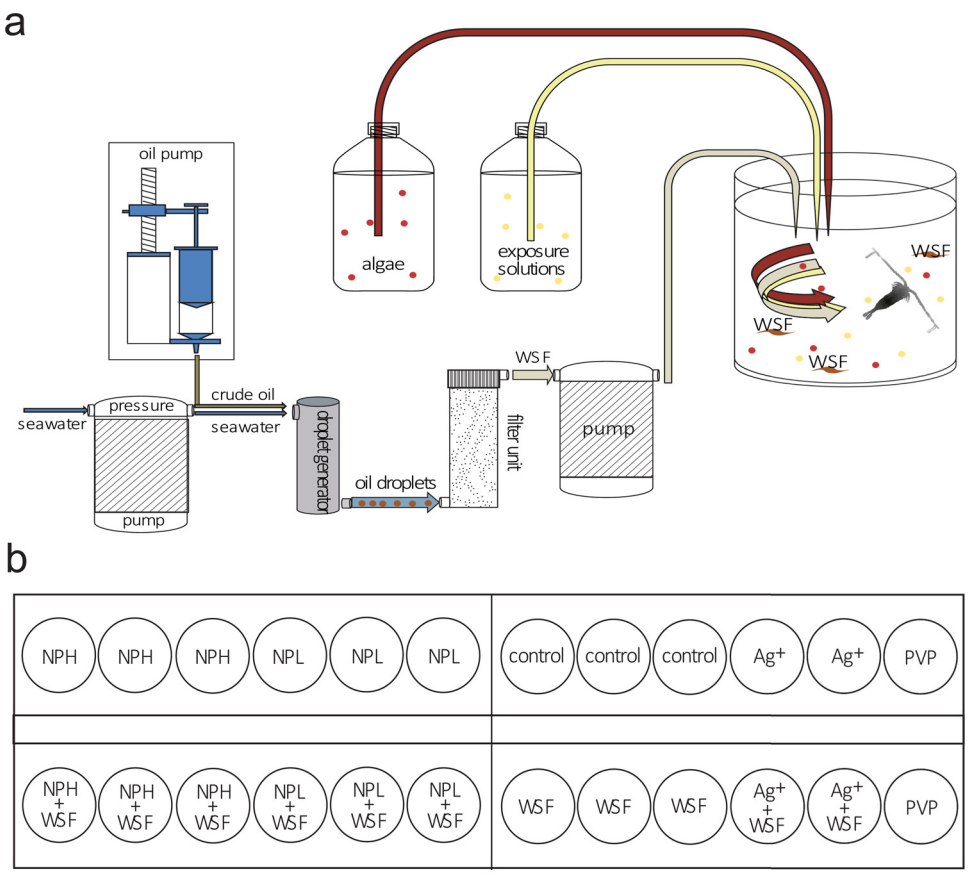

Fig. 1. Schematic of the flow-through system showing (a) the experimental setup with online production of WSF, and (b) exposure tank setup.

effects of the coating material. Exposure stock solutions for AgNP, Ag^+ and PVP were freshly prepared every 12 h, and continuously added to the respective chambers using a tubing pump. The WSF was prepared as described previously (Nordtug et al., 2011) by continuously producing an oil dispersion (2 mg L^{-1} sea water) using a custom-made dispersion generator, and subsequently filtering the dispersion through a filtering unit consisting of loosely packed glass wool (15 g) over GC/C and GC/F filters. The resulting WSF was continuously introduced into the exposure chambers. During the exposure, animals in the individual exposure vessels were fed continuously approximately 4×10^6 cells L^{-1} of the microalgae *Rhodomonas baltica* by a tubing pump. This corresponds to approximately 150 µg L^{-1}. The experiment was conducted at a water and ambient temperature of 10 °C under a 12 h/12 h (dimmed) light/dark regime for 96 h.

2.3.2. Exposure validation

Concentrations of AgNP and Ag^+ were determined in exposure tanks at 0, 24, 72 and 96 h (end) in the flow through experiment as total Ag. Therefore, samples of 10 mL were taken from exposure tanks, stabilized with 0.1 M ultrapure HNO_3 and analyzed using ICP-HR-MS as described above. To determine the exposure concentration of dissolved crude oil components in the WSF, samples of 500 mL were taken from exposure tanks and acidified with 1.3 mL of 37 % HCl for short term storage. No later than 7 days after collection, the samples were adjusted to pH 7 and extracted with pre-conditioned Chromabond® 2000 mg C18/PAH solid phase extraction columns (MachereyNagel, Düren, Germany). Elution of PAHs from SPE column was done with 4 mL acetonitrile – benzene (3:1, v/v). Samples were concentrated to ~1 mL using a gentle stream of N_2 before adding internal standard (fluorene-*d*10). Analyses for semi-volatile organic compounds including decalins, naphthalenes, PAHs and C0-C5 phenols were carried out at SINTEF, Trondheim, Norway as described previously (Faksness et al., 2012). The analytical system comprised an Agilent 7890B GC with an Agilent 5977A quadrupole mass spectrometer. 1 µl of sample was injected into a 310 °C split/splitless injector. The column was an Agilent J&W HP-5MS fused silica capillary column (60 m, 0.25 mm ID, 0.25 µm film thickness). Helium was used as carrier gas with a constant flow of 1.2 mL min^{-1}. MSD ChemStation software was used for data collection and integration. Quantification was performed after normalization to internal standard (fluorene-*d*10) using average relative response factors from a 7-level calibration curve (0.01–2.5 µg/mL). To monitor system performance, a quality control sample (mid-level calibration standard) was run for every 12 sample, and a variation of no more than 25 % was accepted. The analytical limit of detection for each analyte was 0.003 µg mL^{-1}.

2.3.3. Ag uptake in C. finmarchicus

The uptake of total Ag in *C. finmarchicus* was determined after 96 h of exposure to either AgNP and Ag^+ in the flow-through system. Eighty animals were collected from each tank and rinsed in clean seawater before being quickly rinsed twice in deionized water to remove as much as possible of AgNPs attached to the surface of the organisms. Ag concentrations were determined by adding 50 % of purified HNO_3 v/v to the samples prior to digestion in a high-pressure microwave system (Milestone UltraClave, EMLS, Leutkirch, Germany) with a temperature profile increasing gradually from room temperature to 245 °C in 1 h. Final analysis was done by HR-ICP-MS as described above. A small number of individual *C. finmarchicus* were collected from the exposure tanks after 96 h and subjected to coherent anti-Stokes Raman spectroscopy (CARS) to determine (non-quantitatively) the NP attachment on the external surfaces and appendages of the organisms (performed at the University of Exeter, UK) as described in detail in Goodhead et al. (2015).

2.3.4. Gene expression analyses

To determine alterations in gene expression of stress related genes, 20 animals per exposure tank were collected and pooled for analysis. The animals were counted, washed in clean seawater and quickly rinsed twice with filtered deionized water to remove any external Ag particulates. For RNA isolation, whole animals were snap frozen in liquid nitrogen, and were shaken for 2 min with sterile tungsten carbide beads (5 mm; Qiagen) in a Mixer Mill (Retsch, Haan, Germany) before RNA was isolated with TRI Reagent® (Sigma Aldrich, St Louis, Missouri, USA). RNA quality was analyzed with an Experion™ RNA StdSens Analysis Kit (Biorad, CA, USA). Reverse transcription to cDNA was performed using an iScript™ cDNA Synthesis kit (Biorad, Hercules, USA) according to the manufacturer's instructions. Gene expression profiles were analyzed with a C1000 Touch™ Thermal Cycler equipped with CFX96 Touch™ Real-Time PCR Detection System (Bio-Rad, Hercules, USA) using actin as reference gene. Further methodological details and primer sequences are presented in the supporting information (S2.1 Gene expression analysis).

2.3.5. Enzymatic activity

To determine enzymatic activities of the antioxidant enzymes CAT, SOD and GST, 40 animals were sampled, rinsed with seawater, excess water rapidly removed from their surface and pooled. Enzymatic activities were analyzed spectrophotometrically in the post mitochondrial fractions. The pooled samples were homogenized on ice in TRIS buffer (pH 7.6–8 20 mM) containing a protease inhibitor solution (SIGMAFAST™, Sigma-Aldrich/Merck, Darmstadt, Germany), centrifuged twice (10 000*g* for 30 min at 4 °C), and the supernatant collected. Catalase activity (nmol min^{-1} mg^{-1} protein) was determined as peroxidative activity, using a previously described method (Johansson and Borg, 1988). Enzymatic activity of SOD (U mL^{-1} mg $protein^{-1}$) was measured using a SOD assay kit (Sigma-Aldrich/Merck, Darmstadt, Germany). Superoxide dismutase from bovine erythrocytes (2698 U mg^{-1}) was used to quantitatively assess the enzyme activity. GST activity (U mL^{-1} mg $protein^{-1}$) was analyzed using a commercial assay kit (Sigma-Aldrich, St Louis, Missouri, USA). The protein content was determined according to Bradford (Bradford, 1976).

2.4. Statistical analysis

Survival curves and LC_{50} concentrations were generated using GraphPad Prism version 5.0 for Windows (GraphPad Software Inc, La Jolla, CA, USA). Statistical analysis of total Ag uptake, gene expression profiles and enzymatic activities were performed in Statistica 12 (StatSoft, Tulsa, OK, USA). Data were tested for normal distribution and homogeneity of variances before analyzing differences between treatment groups with ANOVA and Duncan's post hoc test. Any data not fulfilling the aforementioned criteria were plotted logarithmically before analysis or, if not reaching criteria, analyzed with Kruskal-Wallis one-way analysis on ranks. Results from exposure groups with only two replicate tanks are reported but were not considered for statistical analysis.

3. Results and discussion

3.1. AgNP characterization

TEM images confirmed that the AgNPs were generally spherical in shape (Fig. 2a). More than 80 % (95 % CI 80.2–100) of the particles were < 20 nm in size (between 1 and 20 nm), with approximately 20 % being larger (27 ± 20 nm) in the stock suspensions (Fig. 2a). The average size (HDD, z-average) of the AgNP in the stock solution was 120 ± 1 nm (PDI 0.27), with a zeta-potential of -21 ± 1 mV.

In seawater, the absorbance of the AgNPs decreased over time (Fig. 2b) indicating a decrease in dispersed AgNPs. The decrease at λ_{max} (403 nm) was 20.8 ± 0.7 % within 1 h and was 63 ± 0.5 % after 12 h. While we detected no spectral shifts, which would indicate a formation of dispersed aggregates, particle aggregation and settling were observed within 12 h (Fig. 2b, c). The results show that AgNP stability was limited in seawater and suggest that AgNP aggregated/agglomerated/dissolved over time. This contrasts with previous studies that reported PVP-coated AgNP to be relatively stable also in seawater (Angel et al., 2013; Khanh and Chen, 2011). However, a similar reduction of λ_{max} of PVP-coated AgNP in seawater was reported by Sikder et al., 2018, and was described to be related to AgNP dissolution. In the current study, the concentration of dissolved Ag present in the AgNP dispersions (445 µg L^{-1}) was on average 90 ± 8 µg L^{-1} (n = 3) and thus accounted on average for 20 % of the Ag concentration present in the AgNP dispersions. AgNP dissolution did not show a significant increase over the 96 h incubation period in seawater, indicating that either further dissolution was limited, or that released Ag^+ formed Ag complexes that were removed from the dissolved fraction by ultracentrifugation and thus not measured as dissolved Ag. A significant initial dissolution, and following reduced Ag^+ release from PVP-coated AgNP in seawater over time was also shown in a previous study (Angel et al., 2013).

3.2. Acute Ag toxicity test

Results of the static acute toxicity tests are shown in Fig. S1. The 96 h LC_{50} concentrations for AgNP were 445 µg L^{-1} (nominal AgNP; CI95 %: 411–481 µg L^{-1}) and 403 µg L^{-1} (total measured Ag; CI95 %: 375–434 µg L^{-1}). For Ag^+ exposures, the LC_{50} was 146 µg L^{-1} Ag^+ (total measured Ag; CI95 %: 135–159 µg L^{-1}). This shows that Ag^+ (applied as $AgNO_3$) was approximately 2.8 times more toxic compared to AgNP, which is in agreement with previous studies (Bilberg et al., 2012; Caballero-Diaz et al., 2013). It is not likely that the higher toxicity is related to the NO_3-N deriving from $AgNO_3$, as tolerable concentrations for marine animals are reported to be around 20 mg L^{-1}, while the maximum NO_3-N concentrations in our study were 0.102 mg L^{-1} (Camargo et al., 2005).

The total determined Ag concentrations decreased approximately 20 % in AgNP exposures during the 96 h exposure, while Ag concentration in the Ag^+ exposures remained stable (data not shown). Together with the dispersion characterization results, this indicates that AgNPs aggregated and sedimented over time. Therefore, despite regular agitation of the exposure vials, AgNP are likely to be removed from the water column and therefore less bioavailable compared to Ag^+, which can, at least partly, explain the lower toxicity in semi-static exposures. It has to be kept in mind that Ag^+ (as in the current study administered as $AgNO_3$ dissolved in de-ionized water) also has a limited stability in seawater and will rapidly form Ag-Cl complexes (e.g. $AgCl_2^-$, $AgCl_3^{2-}$, $AgCl_4^{3-}$), although those can be bioavailable. Further, results from the dissolution studies show that approximately 20 % (90 µg L^{-1}) of the Ag in the AgNP-exposure was present in dissolved form, or as unprecipitated AgCl complexes, which remained stable in seawater during 96 h. It is thus likely that the dissolved Ag from AgNP exposures has contributed to the observed toxicity, especially in the semi-static acute exposure study, as was reported in other studies (Angel et al., 2013; Lee et al., 2018; Navarro et al., 2008). The establishment of LC_{50} concentrations, and comparisons of toxicity between AgNP and Ag^+ remain challenging due to complex metal behavior in seawater including aggregation, dissolution and complexation.

3.3. Combined AgNP-WSF and Ag^+-WSF exposure experiments

3.3.1. Exposure dispersion characterization

The average total Ag concentrations in the exposure tanks were relatively stable throughout the experiment. Average concentrations were 13 and 10 µg L^{-1} for NPL and NPL + WSF, respectively. For the NPH and NPH + WSF the concentrations were 155 and 140 µg L^{-1}, respectively. For, Ag^+ and Ag^+ + WSF the concentrations were 150 and 140 µg L^{-1}, respectively. The total Ag exposure concentrations were

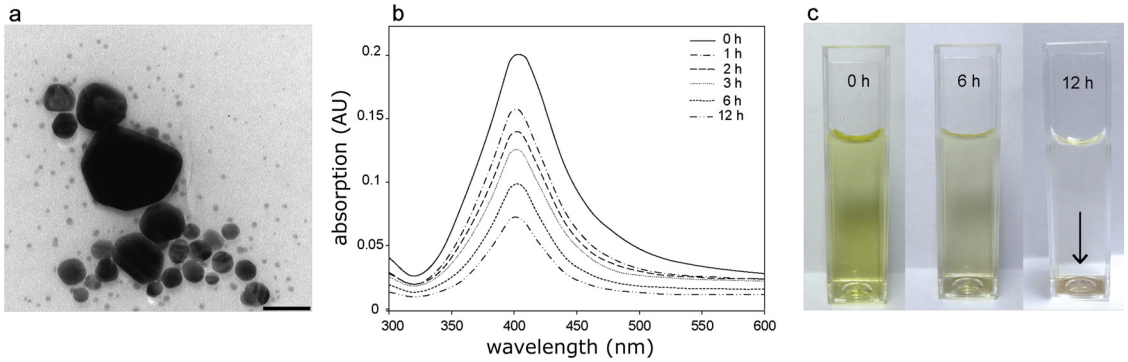

Fig. 2. (a) TEM image of AgNP in MilliQ water, scale bar: 50 nm. (b) absorbance of AgNP in seawater over time. (c) representative images of AgNP aggregation in seawater 0 h, 6 h and 12 h.

thus slightly, but not significantly higher in the NPL, NPH and Ag^+ tanks compared to the total Ag concentrations in the co-exposure tanks (NPL + WSF, NPH + WSF and Ag^+ + WSF). The concentration of total Ag in Ag^+ exposure groups was approximately two times higher than the nominal exposure concentrations. This can be due to either an accumulation of Ag in the exposure tanks or too high concentrations of Ag stock solutions. Interestingly, we did not observe increased mortalities or sublethal responses in the Ag^+ exposure groups, as it could be expected according to the acute toxicity tests. This can be due to the excess presence of algae that where added as feed, as algae can potentially bind or take up Ag and thus reduce free Ag concentrations in the exposure water. Further, fed animals could be more resistant to exposures compared to starved ones in the acute toxicity tests.

Analysis of the WSF composition showed that naphthalenes (57–63 $\mu g\ L^{-1}$) followed by the 2–3 ring PAHs (15–17 $\mu g\ L^{-1}$) were the major constituents in the WSF, NPH + WSF and Ag^+ + WSF exposure tanks (Table S42). Trace levels of naphthalenes and 2–3 ring PAHs were present at detectable levels in the control samples. The total WSF component exposure concentration was slightly higher in the NPH + WSF tanks than in WSF only tanks, although this was not statistically significant (Table S4). The presence of AgNP did not have a measurable influence on the composition of the WSF, confirming that AgNP did not catalyze oxidation or other degradation processes during exposure. This is in contrast to a previous study (Dass et al., 1994) proposing a TiO_2NP mediated photocatalysis of PAHs in water, potentially by the production of hydroxyl radicals on the TiO_2NP surface (Hirano et al., 2005; Xia et al., 2006), which could further react with PAHs and molecular oxygen to ultimately produce PAH-quinone leading to increased toxicity. However, some morphs of TiO_2 are potent photocatalysts, and the ENP-contaminant interactions will likely vary between different ENP materials, coatings, different contaminants and ambient conditions such as light and temperature.

3.3.2. Ag uptake and bioavailability in C. finmarchicus

The total amount of Ag accumulated (analysed after washing the surfaces of the animals) by *C. finmarchicus* was similar following exposure to either AgNP or Ag^+ (Fig. 3a). In NPH and NPH + WSF exposures, Ag concentrations in the animals were significantly higher ($p < 0.001$) compared to NPL and NPL + WSF exposures (Fig. 3a). Ag concentrations were slightly, however, not significantly lower in both WSF co-exposed animals as compared to the animals only exposed to AgNPs (Fig. 3a). Similar accumulation of Ag from AgNP and Ag^+ exposures with similar total Ag concentrations indicate that uptake was probably related to ingestion, potentially via attachment of AgNP and Ag^+ to algae used as food. However, this remains to be investigated in more detail.

CARS imaging showed that AgNP were associated with the external surfaces and appendages of the test organisms, with highest particle attachment observed in the NPH + WSF exposed groups (Fig. 3b). This indicates that the presence of soluble oil components can potentially increase the attachment of AgNP to surfaces, including exposed organisms.

This can be a relevant exposure mechanism also for other ENPs under similar conditions. Quantitative information is not easily obtained from CARS imaging (Goodhead et al., 2015) and the obtained images only allow a qualitative evaluation. Further analyses are thus necessary to quantify this phenomenon.

3.3.3. Gene expression and enzymatic activity

Single and combined exposures of *C. finmarchicus* to AgNP, Ag^+ and WSF caused changes in the gene expression profiles of some of the measured stress related genes (Fig. 4) and the activities of antioxidant enzymes (Fig. 5). However, there was no clear pattern of combined effects in combined versus single exposures. Responses in gene expression were mostly dose dependent in Ag exposures, and were often similar for NPH and Ag^+, which had similar Ag exposure concentrations. Interestingly, while NPH + WSF rather led to slightly higher gene expression responses for most genes as compared to in NPH exposed animals, for the Ag^+ + WSF co-exposed animals, the additional exposure to WSF seemed to cause antagonistic effects, as the expressions of all analysed genes were lower in the Ag^+ + WSF co-exposed animals than in the Ag^+ exposed animals. Nevertheless, the effects of exposure on enzymatic activities were relatively limited. Thus, gene expression analysis seems to be a more sensitive endpoint compared to the measurement of enzymatic activity in the copepod *C. finmarchicus*. Results are discussed in more detail below.

3.3.3.1. SOD gene expression and enzymatic activity. Gene expression of SOD was not significantly impacted by exposure to neither NPL nor NPH relative to the control (NPL or NPH; Fig. 4a). However, a 3-fold higher ($p = 0.018$) SOD gene expression was observed following WSF exposure compared to controls group. The co-exposure to NPH + WSF led to a significantly higher SOD gene expression response than observed for the NPL-WSF and NPH groups, while SOD gene expression was statistically similar in WSF and NPH + WSF exposures (Fig. 4a).

In contrast to gene expression, we detected a reduction in SOD enzymatic activity for several exposure conditions including PVP, which was significant for NPL ($p = 0.046$) (Fig. 5a). This can potentially be due to an inhibition of the SOD enzyme by the contaminant exposures, and an increased gene expression as compensation reaction. An inhibition of SOD gene expression and enzymatic activity in brain of AgNP exposed fish (*Tilapia zilii*) was described previously (Afifi et al., 2016). Hansen et al. (2017) did not find increased SOD enzymatic activity in *C. finmarchicus* following exposure to oxidative stress in the form of H_2O_2 exposure (Hansen et al., 2017).

3.3.3.2. CAT gene expression and enzymatic activity. Although AgNP has

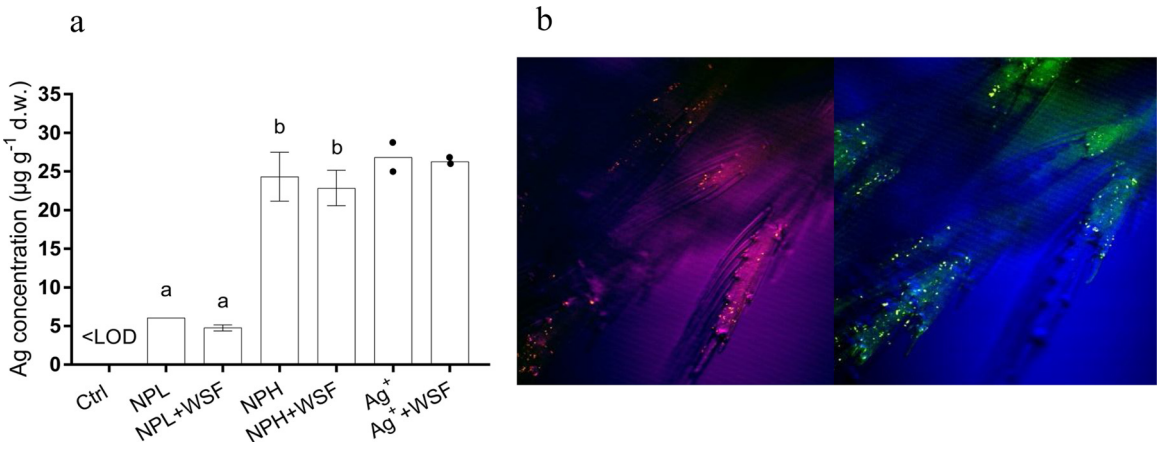

Fig. 3. a) Total Ag concentrations in *C. finmarchicus* after 96 h of flow through exposure to AgNP and Ag^+ in the presence and absence of WSF. Data are presented as mean ± Stdev for the AgNP and AgNP + WSF exposure groups and as mean ± min, max (filled circles) for the Ag^+, Ag^+ + WSF exposure groups. Different lowercase letters indicate statistically significant differences ($p < 0.05$) between groups. b) CARS images of *C. finmarchicus* after 96 h of flow through exposure to AgNP + WSF (NPH) showing AgNP and AgNP aggregate attachment to the legs of the organism.

previously been reported to cause oxidative stress in exposed organisms and cells (Ahamed et al., 2010; Buffet et al., 2014), none of the single pollutant exposures or their mixtures elicited a significant response in CAT gene expression levels in exposed *C. finmarchicus* in this study (Fig. 4b). Neither were any differences in enzymatic activity observed in exposed groups in comparison to controls (Fig. 5b). Similarly, previous studies reported that CAT was less sensitive to AgNPs in comparison to the other ROS scavenging enzymes (Buffet et al., 2014; Massarsky et al., 2014; McCarthy et al., 2013). Further, no activation of CAT enzymatic activity was discovered in *C. finmarchicus* following the exposure to H_2O_2, which is the substrate for the CAT enzyme (Hansen et al., 2017). This indicates that CAT is probably not one of the copepods major oxidative stress defence mechanisms in these copepods and not suitable as biomarker for oxidative stress in *C. finmarchicus*.

3.3.3.3. GST gene expression and enzymatic activity. GST gene expression was upregulated in all high Ag exposures. Up-regulation was 3-fold in NPH exposures ($p = 0.0093$) relative to NPL and the control (Fig. 4c) and was also significantly higher in NPH-WSF ($p = 0.0019$) relative to controls. The co-exposure NPH-WSF did cause a higher response compared to NPH, which resembled an additive effect. This was, however, not observed for NPL + WSF.

GST enzyme activity was significantly higher in both NPL ($p = 0.0177$) and NPH ($p = 0.0053$) exposures as compared to the control group (Fig. 5c). The presence of the WSF did not cause consistent mixture effects, as WSF decreased enzymatic activity, but increased gene expression was observed in NPH + WSF and Ag^+ + WSF, but not in NPL + WSF (Fig. 5c). Hansen et al. (2017) reported a slight increase in GST enzymatic activity following H_2O_2 exposure. Similarly, increased transcription following exposure to WSFs of crude oils and marine fuel oils were previously described (Hansen et al., 2009). In the current study we found GST being especially responsive to Ag exposures, with slight, but insignificant responses in GST transcription following WSF exposure. Difference in findings may be caused by difference in exposure concentration and duration.

3.3.3.4. HSP90 and CYP330A1 gene expression. Results show that high AgNP exposures increased the transcription of both HSP90 ($p = 0.0487$) and CYP330A1 after 96 h exposure ($p = 0.0408$) (Fig. 4d, e). Similarly, HSP90 expression was significantly higher in NPH + WSF ($p = 0.0443$) compared to controls, however, there was no differences compared to AgNP-only exposure (Fig. 4d).

In contrast, co-exposures of NPH + WSF resulted in lower gene expression levels of CYP330A1 compared to single NPH exposures ($p = 0.0466$). This is in line with previous studies of CYP330A1, an enzyme suggested to be involved in crustacean ecdysteroid biosynthesis and lipid turnover (Hansen et al., 2008), where reduced expression has been shown in *C. finmarchicus* after exposure to naphthalene (Hansen et al., 2008), oil dispersion and WSF (Hansen et al., 2009). A similar trend was seen for NPL and Ag^+ exposures compared to the combined exposures.

3.3.4. Combined effects

Taken together, there is no clear overall pattern of combined contaminant effects in this study. On a gene expression level, as compared to the control group, the co-exposure of NPH + WSF seemed to cause (slightly) higher responses in SOD and GST, while Ag^+ + WSF caused lower responses for almost all measured endpoints, compared to Ag^+ alone, with no major responses observed in NPL or NPL + WSF exposed animals. In line with the decreased response to combined Ag^+ + WSF treatment, the uptake of Ag was slightly decreased in combined exposures. In Ag^+ + WSF exposed groups this could contribute to the observed decreased effects. While Ag uptake also slightly decreased in AgNP + WSF groups, this was not reflected in the effect responses, probably due to the increased attachment of AgNP to the animals surfaces in the presence of WSF (Fig. 3a, b). Due to the limited availability of samples, differences in uptake/accumulation of oil components in *C. finmarchicus* were not measured in the current study, but should be included in future in order to determine whether the presence of AgNP or Ag^+ plays a role for the bioavailability of oil components.

Findings on the combined effects of ENPs and contaminants vary from increased to decreased toxicity and seem to be dependent on the interaction of ENPs and contaminants (Naasz et al., 2018).

A study on the combined effects of 17α-ethinylestradiol (EE2) and AgNP on the freshwater mudsnail *Potamopyrgus antipodarum* (28-day exposure duration) showed that AgNP can increase the effects of EE2 on reproduction at no-effect doses of EE2. In contrast, the same study reported that AgNP reduced the impact of EE2 at endocrinological active concentrations (Volker et al., 2014). Magesky and Pelletier (2015) reported complex interactions and effects of Ag^+, AgNP and SWCNT on early developmental stages of sea urchins. A recent study on combined effects of AgNP and As, Cr and Cd on a the oxidative stress response and gene expression pattern in a human cell line, and reported different combined mode of combined actions, with synergistic effects reported AgNP + As and AgNP + Cd and additive effects on AgNP + Cr (Fukushima et al., 2020).

Other studies reported combined effects of ENP such as TiO_2NP and carbon nanomaterials with contaminants that range from facilitated

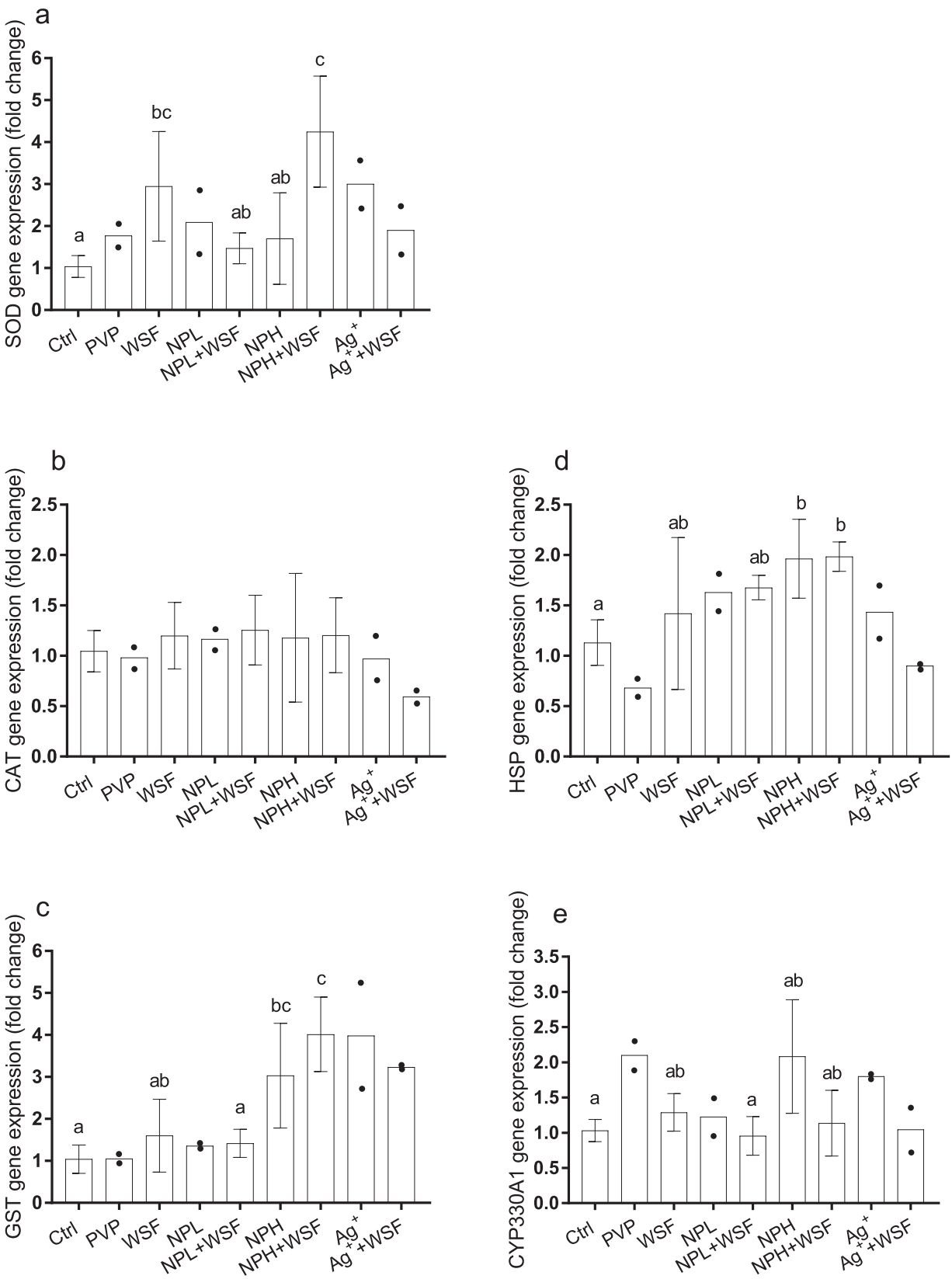

Fig. 4. Gene expression of (a) SOD, (b) CAT, (c) GST, (d) HSP90 and (e) CYP330A1 in *C. finmarchicus* after 96 h of flow through exposure to AgNP (NPL and NPH), Ag^+ and respective mixtures with WSF (NPL-WSF and NPH-WSF). Data are presented as mean ± Stdev for AgNP and AgNP + WSF exposure groups and as mean ± upper and lower value (closed circles) for Ag^+ and Ag^+ + WSF exposure groups, as those consisted of only 2 replicates. These were also not considered for statistical analyses. In other groups, different letters indicate significant differences between groups ($p < 0.05$).

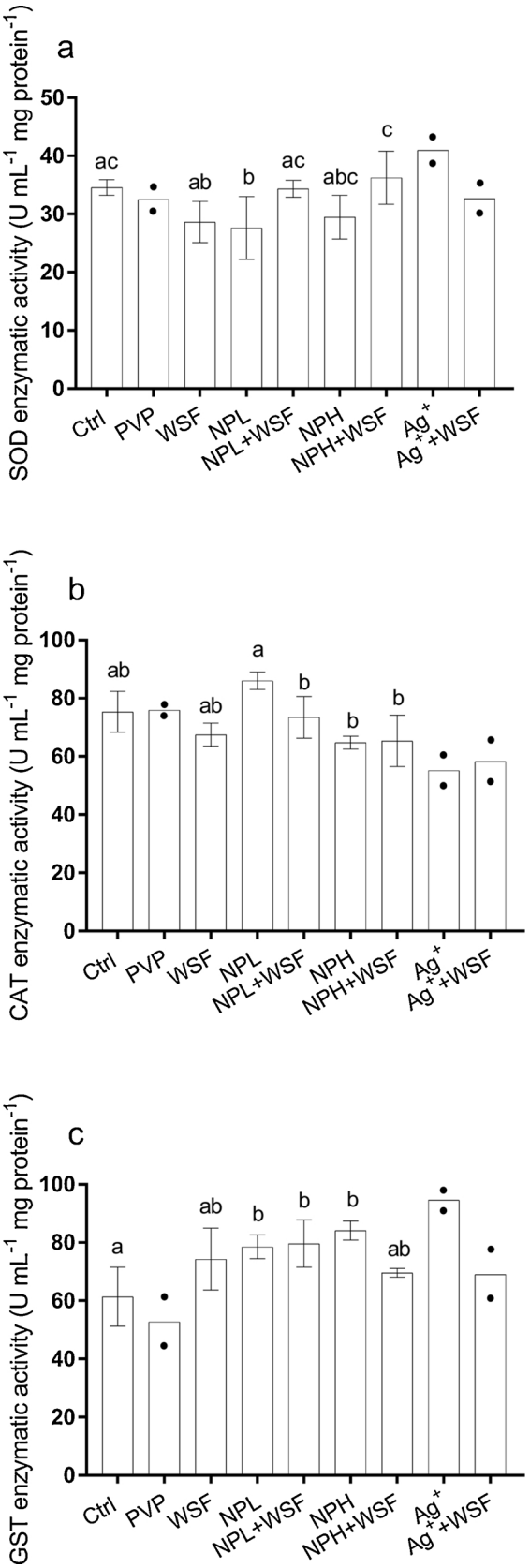

Fig. 5. Enzymatic activity of exposed *C. finmarchicus* (a) SOD, (b) CAT and (c) GST. Data are presented as mean ± Stdev for AgNP (NPL and NPH) and AgNP + WSF (NPL and NPH) exposure groups, and as mean ± min, max (closed circles) for Ag^+ and Ag^+ + WSF exposure groups, as those consisted of only 2 replicates. These were also not considered for statistical analyses. In other groups, different letters indicate significant differences between groups ($p < 0.05$).

transport to synergistic or antagonistic effects depending on the studied ENP and biomarker investigated:

An increased contaminant uptake, and a resulting enhanced toxicity, was shown for the organic pollutants tetrachlorodibenzodioxin (TCDD) and tributyltin (TBT) in marine molluscs (*Mytilus galloprovincialis* and *Haliotis diversicolor supertexta*) in the presence of titanium dioxide TiO_2NP (Canesi et al., 2014; Zhu et al., 2011). Further, TiO_2NP was shown to enhance the uptake and toxicity of arsenic and cadmium in common carp (*Cyprinus carpio*) (Sun et al., 2007; Zhang et al., 2007). Enhanced toxic effects such as DNA damage of benzo(a)pyrene were also reported in the presence of TiO_2NP in *Mytilus edulis* (Farkas et al., 2015).

4. Conclusions

In the current study, we showed that Ag is toxic to *C. finmarchicus* in both ionic and nanoparticulate form. Generally, combined effects of AgNPs and the WSF of crude oil on the calanoid copepod *C. finmarchicus* seem to be limited under the studied conditions.

This complex field needs to be studied in more detail, using systematic approaches to determine ENP-chemical interactions, attempt to relate ENP and chemical properties to inter-reactivity and relate interaction with bioavailability and toxicity.

CRediT authorship contribution statement

J. Farkas: Conceptualization, Validation, Investigation, Writing - original draft, Writing - review & editing, Visualization, Supervision, Project administration, Funding acquisition, Formal analysis. **V. Cappadona:** Validation, Investigation, Writing - original draft, Formal analysis. **A.J. Olsen:** Conceptualization, Investigation, Supervision, Funding acquisition. **B.H. Hansen:** Writing - original draft. **W. Posch:** Investigation, Writing - original draft, Resources. **T.M. Ciesielski:** Conceptualization, Investigation, Funding acquisition, Formal analysis. **R. Goodhead:** Investigation. **D. Wilflingseder:** Writing - original draft, Resources. **M. Blatzer:** Investigation, Writing - review & editing, Formal analysis. **D. Altin:** Investigation. **Julian Moger:** Methodology, Resources. **A.M. Booth:** Writing - original draft. **B.M. Jenssen:** Conceptualization, Writing - original draft, Funding acquisition.

Declaration of Competing Interest

The authors declare that they have no known competing financial interests or personal relationships that could have appeared to influence the work reported in this paper.

Acknowledgements

The work presented in this paper has been funded through the Research Council of Norway project NANOMARINE (grant number 216464/E40). The authors wish to thank the RCN for their financial support. In addition, we want to acknowledge Syverin Lierhagen for invaluable help with ICP-MS analyses.

Appendix A. Supplementary data

Supplementary material related to this article can be found, in the online version, at doi:https://doi.org/10.1016/j.aquatox.2020.105582.

References

Afifi, M., Saddick, S., Abu Zinada, O.A., 2016. Toxicity of silver nanoparticles on the brain of Oreochromis niloticus and Tilapia zillii. Saudi J. Biol. Sci. 23, 754–760.

Ahamed, M., Posgai, R., Gorey, T.J., Nielsen, M., Hussain, S.M., Rowe, J.J., 2010. Silver nanoparticles induced heat shock protein 70, oxidative stress and apoptosis in Drosophila melanogaster. Toxicol. Appl. Pharm. 242, 263–269.

Angel, B.M., Batley, G.E., Jarolimek, C.V., Rogers, N.J., 2013. The impact of size on the fate and toxicity of nanoparticulate silver in aquatic systems. Chemosphere 93, 359–365.
Baun, A., Sorensen, S.N., Rasmussen, R.F., Hartmann, N.B., Koch, C.B., 2008. Toxicity and bioaccumulation of xenobiotic organic compounds in the presence of aqueous suspensions of aggregates of nano-C(60). Aquat. Toxicol. 86, 379–387.
Benn, T.M., Westerhoff, P., 2008. Nanoparticle silver released into water from commercially available sock fabrics. Environ. Sci. Technol. 42, 4133–4139.
Bilberg, K., Hovgaard, M.B., Besenbacher, F., Baatrup, E., 2012. In vivo toxicity of silver nanoparticles and silver ions in zebrafish (Danio rerio). J. Toxicol. 2012 293784.
Bradford, M.M., 1976. A rapid and sensitive method for the quantitation of microgram quantities of protein utilizing the principle of protein-dye binding. Anal. Biochem. 72, 248–254.
Buffet, P.E., Zalouk-Vergnoux, A., Chatel, A., Berthet, B., Metais, I., Perrein-Ettajani, H., Poirier, L., Luna-Acosta, A., Thomas-Guyon, H., Risso-de Faverney, C., Guibbolini, M., Gilliland, D., Valsami-Jones, E., Mouneyrac, C., 2014. A marine mesocosm study on the environmental fate of silver nanoparticles and toxicity effects on two endobenthic species: The ragworm Hediste diversicolor and the bivalve mollusc Scrobicularia plana. Sci. Total Environ. 470, 1151–1159.
Caballero-Diaz, E., Pfeiffer, C., Kastl, L., Rivera-Gil, P., Simonet, B., Valcarcel, M., Jimenez-Lamana, J., Laborda, F., Parak, W.J., 2013. The toxicity of silver nanoparticles depends on their uptake by cells and thus on their surface chemistry. Part. Part. Syst. Charact. 30, 1079–1085.
Camargo, J.A., Alonso, A., Salamanca, A., 2005. Nitrate toxicity to aquatic animals: a review with new data for freshwater invertebrates. Chemosphere 58, 1255–1267.
Canesi, L., Frenzilli, G., Balbi, T., Bernardeschi, M., Ciacci, C., Corsolini, S., Della Torre, C., Fabbri, R., Faleri, C., Focardi, S., Guidi, P., Kocan, A., Marcomini, A., Mariottini, M., Nigro, M., Pozo-Gallardo, K., Rocco, L., Scarcelli, V., Smerilli, A., Corsi, I., 2014. Interactive effects of n-TiO2 and 2,3,7,8-TCDD on the marine bivalve Mytilus galloprovincialis. Aquat. Toxicol. 153, 53–65.
Dankovich, T.A., Gray, D.G., 2011. Bactericidal paper impregnated with silver nanoparticles for point-of-use water treatment. Environ. Sci. Technol. 45, 1992–1998.
Dass, S., Muneer, M., Godpidas, K.R., 1994. Photocatalytic degradation of wastewater pollutants. Titanium-dioxide-mediated oxidation of polynuclear aromatic hydrocarbons. J. Photochem. Photobiol. A: Chem. 77, 83–88.
Deng, R., Lin, D., Zhu, L., Majumdar, S., White, J.C., Gardea-Torresdey, J.L., Xing, B., 2017. Nanoparticle interactions with co-existing contaminants: joint toxicity, bioaccumulation and risk. Nanotoxicology 11, 591–612.
Faksness, L.G., Hansen, B.H., Altin, D., Brandvik, P.J., 2012. Chemical composition and acute toxicity in the water after in situ burning – a laboratory experiment. Mar. Pollut. Bull. 64, 49–55.
Falkner, R., Jaspers, N., 2012. Regulating nanotechnologies: risk, uncertainty and the global governance gap. Glob. Environ. Polit. 12, 30–55.
Farkas, J., Peter, H., Christian, P., Gallego Urrea, J.A., Hassellov, M., Tuoriniemi, J., Gustafsson, S., Olsson, E., Hylland, K., Thomas, K.V., 2011. Characterization of the effluent from a nanosilver producing washing machine. Environ. Int. 37, 1057–1062.
Farkas, J., Bergum, S., Nilsen, E.W., Olsen, A.J., Salaberria, I., Ciesielski, T.M., Baczek, T., Konieczna, L., Salvenmoser, W., Jenssen, B.M., 2015. The impact of TiO2 nanoparticles on uptake and toxicity of benzo(a)pyrene in the blue mussel (Mytilus edulis). Sci. Total Environ. 511, 469–476.
Farkas, J., Salaberria, I., Styrishave, B., Staňková, R., Ciesielski, T.M., Olsen, A.J., Posch, W., Flaten, T.P., Krøkje, Å., Salvenmoser, W., Jenssen, B.M., 2017. Exposure of juvenile turbot (Scophthalmus maximus) to silver nanoparticles and 17α-ethinylestradiol mixtures: implications for contaminant uptake and plasma steroid hormone levels. Environ. Pollut. 220, 328–336.
Farmen, E., Mikkelsen, H.N., Evensen, O., Einset, J., Heier, L.S., Rosseland, B.O., Salbu, B., Tollefsen, K.E., Oughton, D.H., 2012. Acute and sub-lethal effects in juvenile Atlantic salmon exposed to low mug/L concentrations of Ag nanoparticles. Aquat. Toxicol. 108, 78–84.
Fukushima, T., Jintana, W., Okabe, S., 2020. Mixture toxicity of the combinations of silver nanoparticles and environmental pollutants. Environ. Sci. Pollut. Res. - Int. 27, 6326–6337.
Glomstad, B., Altin, D., Sørensen, L., Liu, J., Jenssen, B.M., Booth, A.M., 2016. Carbon nanotube properties influence adsorption of phenanthrene and subsequent bioavailability and toxicity to Pseudokirchneriella subcapitata. Environ. Sci. Technol. 50, 2660–2668.
Goodhead, R.M., Moger, J., Galloway, T.S., Tyler, C.R., 2015. Tracing engineered nanomaterials in biological tissues using coherent anti-Stokes Raman scattering (CARS) microscopy – a critical review. Nanotoxicology 9, 928–939.
Hadrup, N., Sharma, A.K., Loeschner, K., 2018. Toxicity of silver ions, metallic silver, and silver nanoparticle materials after in vivo dermal and mucosal surface exposure: a review. Regul. Toxicol. Pharmacol. 98, 257–267.
Hansen, B.H., Altin, D., Nordtug, T., Olsen, A.J., 2007. Suppression subtractive hybridization library prepared from the copepod Calanus finmarchicus exposed to a sublethal mixture of environmental stressors. Comp. Biochem. Physiol. Part D Genomics Proteomics 2, 250–256.
Hansen, B.H., Altin, D., Vang, S.H., Nordtug, T., Olsen, A.J., 2008. Effects of naphthalene on gene transcription in Calanus finmarchicus (Crustacea: Copepoda). Aquat. Toxicol. 86, 157–165.
Hansen, B.H., Hallmann, A., Altin, D., Jenssen, B.M., Ciesielski, T.M., 2017. Acute hydrogen peroxide (H2O2) exposure does not cause oxidative stress in late-copepodite stage of Calanus finmarchicus. J. Toxicol. Environ. Health A 80, 820–829.
Hansen, B.H., Nordtug, T., Altin, D., Booth, A., Hessen, K.M., Olsen, A.J., 2009. Gene expression of GST and CYP330A1 in lipid-rich and lipid-poor female Calanus finmarchicus (Copepoda: Crustacea) exposed to dispersed oil. J. Toxicol. Environ. Health, Part A 72 (3–4), 131–139.
Hartmann, N.B., Baun, A., 2010. The nano cocktail: ecotoxicological effects of engineered nanoparticles in chemical mixtures. Integr. Environ. Assess. Manag. 6, 311–313. https://doi.org/10.1002/ieam.39.
Hirano, K., Nitta, H., Sawada, K., 2005. Effect of sonication on the photo-catalytic mineralization of some chlorinated organic compounds. Ultrason. Sonochem. 12, 271–276.
Johansson, L.H., Borg, L.A.H., 1988. A spectrophotometric method for determination of catalase activity in small tissue samples. Anal. Biochem. 174, 331–336.
Khanh, A.H., Chen, K.L., 2011. Aggregation kinetics of citrate and polyvinylpyrrolidone coated silver nanoparticles in monovalent and divalent electrolyte solutions. Environ. Sci. Technol. 45 (13), 5564–5571.
Lee, W.S., Kim, E., Cho, H.-J., Kang, T., Kim, B., Kim, M.Y., Kim, Y.S., Song, N.W., Lee, J.-S., Jeong, J., 2018. The relationship between dissolution behavior and the toxicity of silver nanoparticles on zebrafish embryos in different ionic environments. Nanomaterials (Basel) 8, 652.
Li, D., Hong, B., Fang, W., Guo, Y., Lin, R., 2010. Preparation of well-dispersed silver nanoparticles for oil-based nanofluids. Ind. Eng. Chem. Res. 49, 1697–1702.
Magesky, A., Pelletier, E., 2015. Toxicity mechanisms of ionic silver and polymer-coated silver nanoparticles with interactions of functionalized carbon nanotubes on early development stages of sea urchin. Aquat. Toxicol. 167, 106–123.
Massarsky, A., Abraham, R., Nguyen, K.C., Rippstein, P., Tayabali, A.F., Trudeau, V.L., Moon, T.W., 2014. Nanosilver cytotoxicity in rainbow trout (Oncorhynchus mykiss) erythrocytes and hepatocytes. Comp. Biochem. Phys. C 159, 10–21.
McCarthy, M.P., Carroll, D.L., Ringwood, A.H., 2013. Tissue specific responses of oysters, Crassostrea virginica, to silver nanoparticles. Aquat. Toxicol. 138, 123–128.
Mueller, N., Nowack, B., 2008. Exposure modeling of engineered nanoparticles in the environment. Environ. Sci. Technol. 42, 4447–4453.
Naasz, S., Altenburger, R., Kühnel, D., 2018. Environmental mixtures of nanomaterials and chemicals: the Trojan-horse phenomenon and its relevance for ecotoxicity. Sci. Total Environ. 635, 1170–1181.
Navarro, E., Piccapietra, F., Wagner, B., Marconi, F., Kaegi, R., Odzak, N., Sigg, L., Behra, R., 2008. Toxicity of silver nanoparticles to Chlamydomonas reinhardtii. Environ. Sci. Technol. 42, 8959–8964.
Nordtug, T., Olsen, A.J., Altin, D., Meier, S., Overrein, I., Hansen, B.H., Johansen, O., 2011. Method for generating parameterized ecotoxicity data of dispersed oil for use in environmental modelling. Mar. Pollut. Bull. 62, 2106–2113.
Park, C.B., Jung, J.W., Baek, M., Sung, B., Park, J.W., Seol, Y., Yeom, D.H., Park, J.W., Kim, Y.J., 2019. Mixture toxicity of metal oxide nanoparticles and silver ions on Daphnia magna. J. Nanoparticle Res. 21, 166.
Ribeiro, F., Gallego-Urrea, J.A., Jurkschat, K., Crossley, A., Hassellov, M., Taylor, C., Soares, A.M., Loureiro, S., 2014. Silver nanoparticles and silver nitrate induce high toxicity to Pseudokirchneriella subcapitata, Daphnia magna and Danio rerio. Sci. Total Environ. 466–467, 232–241.
Rosenfeldt, R.R., Seitz, F., Schulz, R., Bundschuh, M., 2014. Heavy metal uptake and toxicity in the presence of titanium dioxide nanoparticles: a factorial approach using daphnia magna. Environ. Sci. Technol. 48 (12), 6965–6972.
Rosenfeldt, R.R., Seitz, F., Zubrod, J.P., Feckler, A., Merkel, T., Luederwald, S., Bundschuh, R., Schulz, R., Bundschuh, M., 2015. Does the presence of titanium dioxide nanoparticles reduce copper toxicity? A factorial approach with the benthic amphipod Gammarus fossarum. Aquat. Toxicol. 165, 154–159.
Sakshaug, E., Bjørge, A., Gulliksen, B., Loeng, H., Mehlum, F., 1992. Økosystem Barentshavet (in Norwegian). Universitetsforlaget, Oslo.
Sikder, M., Lead, J.R., Chandler, T.G., Baalousha, M., 2018. A rapid approach for measuring silver nanoparticle concentration and dissolution in seawater by UV–Vis. Sci. Total Environ. 597–607.
Sun, H.W., Zhang, X.Z., Niu, Q., Chen, Y.S., Crittenden, J.C., 2007. Enhanced accumulation of arsenate in carp in the presence of titanium dioxide nanoparticles. Water Air Soil Pollut. Focus. 178, 245–254.
Sun, X.-F., Qin, J., Xia, P.-F., Guo, B.-B., Yang, C.-M., Song, C., Wang, S.-G., 2015. Graphene oxide–silver nanoparticle membrane for biofouling control and water purification. Chem. Eng. J. 281, 53–59.
Volker, C., Graf, T., Schneider, I., Oetken, M., Oehlmann, J., 2014. Combined effects of silver nanoparticles and 17alpha-ethinylestradiol on the freshwater mudsnail Potamopyrgus antipodarum. Environ. Sci. Pollut. Res. Int. 21, 10661–10670.
Warheit, D., 2018. Hazard and risk assessment strategies for nanoparticle exposures: how far have we come in the past 10 years? [version 1; referees: 2 approved]. F1000Research 7.
Xia, T., Kovochich, M., Brant, J., Hotze, M., Sempf, J., Oberley, T., Sioutas, C., Yeh, J.I., Wiesner, M.R., Nel, A.E., 2006. Comparison of the abilities of ambient and manufactured nanoparticles to induce cellular toxicity according to an oxidative stress paradigm. Nano Lett. 6, 1794–1807.
Zhang, X., Sun, H., Zhang, Z., Niu, Q., Chen, Y., Crittenden, J.C., 2007. Enhanced bioaccumulation of cadmium in carp in the presence of titanium dioxide nanoparticles. Chemosphere 67, 160–166.
Zhu, X., Zhou, J., Cai, Z., 2011. TiO2 nanoparticles in the marine environment: impact on the toxicity of tributyltin to abalone (Haliotis diversicolor supertexta) embryos. Environ. Sci. Technol. 45, 3753–3758.